We are IntechOpen, the world's leading publisher of Open Access books Built by scientists, for scientists

4,800
Open access books available

122,000
International authors and editors

135M
Downloads

Our authors are among the

154
Countries delivered to

TOP 1%
most cited scientists

12.2%
Contributors from top 500 universities

CLARIVATE ANALYTICS BOOK CITATION INDEX INDEXED

WEB OF SCIENCE™

Selection of our books indexed in the Book Citation Index in Web of Science™ Core Collection (BKCI)

Interested in publishing with us?
Contact book.department@intechopen.com

Numbers displayed above are based on latest data collected.
For more information visit www.intechopen.com

23

Robust Current Controller Considering Position Estimation Error for Position Sensor-less Control of Interior Permanent Magnet Synchronous Motors under High-speed Drives

Masaru Hasegawa and Keiju Matsui
Chubu University University
Japan

1. Introduction

This paper proposes a new current controller for high-speed drives of position sensor-less controlled Interior Permanent Magnet Synchronous Motors (IPMSMs).
Recent demands of motor drive systems are

1. improved efficiency,
2. high torque response,
3. minimum motor size,
4. low cost.

IPMSMs and vector control are widely utilized because of thier efficiency(1) and high torque response(2). In addition, much attention about high speed motors has been attracted from the viewpoint of (3) because the high speed operation makes it possible to achieve smaller motor size for specialized applications such as electric vehicles and home appliances, and so on. High-performance digital control processors cannot be employed to achieve low cost system(4), however, so lower cut-off frequency needs to be achieved because the relatively long control period(– often 500μs to 1ms –) is required. In this situation, the conventional current control system for an IPMSM often degrades and violates stability of the system.
In high-speed drives of AC motors, it has been pointed out that unstable current control tends to occur since coupling terms based on electromotive force impair the characteristics of current control (J.Jung & K.Nam (1999), K.Kondo et al. (1998 (in Japanese)). These papers have proposed a new dynamic decoupling controller, respectively, under the assumption that the controller's coordinate ($\gamma - \delta$) is perfectly aligned with the rotating coordinate fixed to the rotor magnet or rotor flux($d - q$). Hence, it is easily expected that this instability problem tends to be emphasized when position error between these coordinates occurs, which is often visible in the case of position sensor-less control.
In this paper, stability analysis is carried out while considering its application to position sensor-less system (Z.Chen et al. (2003), S.Morimoto et al. (2002), M.Hasegawa & K.Matsui (2008)) , and stable regions are clarified, in which it is especially difficult to control currents on synchronous reference frame at high-speed (K.Tobari et al. (2004 (in Japanese)) . In order

to solve this instability, a simply modified current controller is proposed in this paper. To guarantee both robust stability and current control performance simultaneously, this paper employees two degree of freedom (2DOF) structure fot the current controller, which can enlarge stable region and maintain its performance (Hasegawa et al. (2007)). Finally, some experiments with a disturbance observer for sensor-less control show that the proposed current controller is effective to enlarge high-speed drives for IPMSM sensor-less system.

2. IPMSM model and conventional controller design

IPMSM on the rotational reference coordinate synchronized with the rotor magnet ($d-q$ axis) can be expressed by

$$\begin{bmatrix} v_d \\ v_q \end{bmatrix} = \begin{bmatrix} R + pL_d & -P\omega_{rm}L_q \\ P\omega_{rm}L_d & R + pL_q \end{bmatrix} \begin{bmatrix} i_d \\ i_q \end{bmatrix} + \begin{bmatrix} 0 \\ P\omega_{rm}K_E \end{bmatrix} , \tag{1}$$

in which R means winding resistance, and L_d and $_q$ stand for inductances in d-q axes. ω_{rm} and P express motor speed in mechanical angle and the number of pole pairs, respectively.
In conventional current controller design, the following decoupling controller is usually utilized to independently control d axis current and q axis current:

$$v_d^* = v_d' - P\omega_{rm}L_q i_q , \tag{2}$$

$$v_q^* = v_q' + P\omega_{rm}(L_d i_d + K_E) , \tag{3}$$

where v_d' and v_q' are obtained by amplifying current control errors with proportional - integral controllers to regulate each current to the desired value, as follows:

$$v_d' = \frac{K_{pd}s + K_{id}}{s}(i_d^* - i_d) , \tag{4}$$

$$v_q' = \frac{K_{pq}s + K_{iq}}{s}(i_q^* - i_q) , \tag{5}$$

in which x^* means reference of x. From (1) to (5), feed-back loop for i_d and i_q is constructed, and current controller gains are often selected as follows:

$$K_{pd} = \omega_c L_d , \tag{6}$$

$$K_{id} = \omega_c R , \tag{7}$$

$$K_{pq} = \omega_c L_q , \tag{8}$$

$$K_{iq} = \omega_c R , \tag{9}$$

where ω_c stands for the cut-off frequency for current control. Therefore, the stability of the current control system can be guaranteed, and these PI controllers can play a role in eliminating slow dynamics of current control by cancelling the poles of motor winding ($= -\frac{R}{L_d}, -\frac{R}{L_q}$) by the zero of controllers.
It should be noted, however, that extremely accurate measurement of the rotor position must be assumed to hold this discussion and design because these current controllers are designed and constructed on $d-q$ axis. Hence, the stability of the current control system would easily be violated when the current controller is constructed on $\gamma-\delta$ axis if there exists position error $\Delta\theta_{re}$ (see Fig. 1) due to the delay of position estimation and the parameter mismatches in position sensor-less control system. The following section proves that the instability especially tends to occur in high-speed regions when synchronous motors with large $L_d - L_q$ are employed.

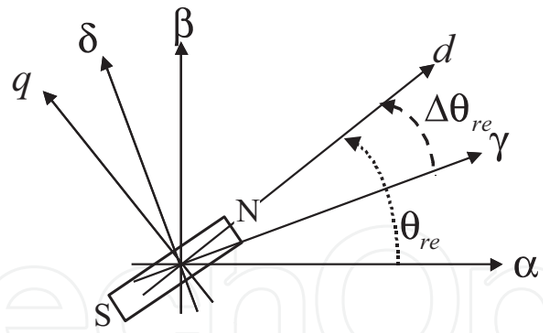

Fig. 1. Coordinates for IPMSMs

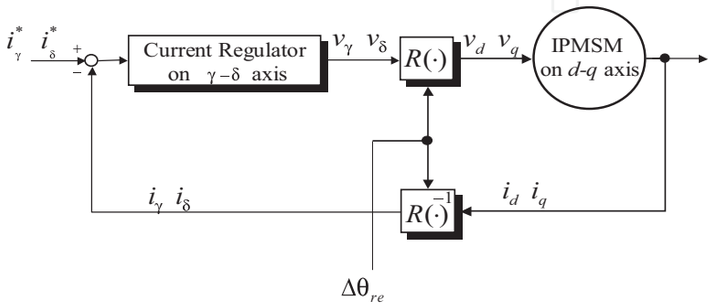

Fig. 2. Control system in consideration of position estimation error

3. Stability analysis of current control system

3.1 Problem Statement

This section analyses stability of current control system while considering its application to position sensor-less system. Let $\gamma - \delta$ axis be defined as a rectangular coordinate away from $d - q$ axis by position error $\Delta\theta_{re}$ shown in Fig.1. This section investigates the stability of the current control loop, which consists of IPMSM and current controller on $\gamma - \delta$ axis as shown in Fig.2.

From (1), IPMSM on $\gamma - \delta$ axis can be rewritten as

$$\begin{bmatrix} v_\gamma \\ v_\delta \end{bmatrix} = \begin{bmatrix} R - P\omega_{rm}L_{\gamma\delta} + L_\gamma p & -P\omega_{rm}L_\delta + L_{\gamma\delta}p \\ P\omega_{rm}L_\gamma + L_{\gamma\delta}p & R + P\omega_{rm}L_{\gamma\delta} + L_\delta p \end{bmatrix} \begin{bmatrix} i_\gamma \\ i_\delta \end{bmatrix} + P\omega_{rm}K_E \begin{bmatrix} -\sin\Delta\theta_{re} \\ \cos\Delta\theta_{re} \end{bmatrix}, \tag{10}$$

in which

$$\begin{aligned} L_\gamma &= L_d - (L_d - L_q)\sin^2\Delta\theta_{re}\,, \\ L_\delta &= L_q + (L_d - L_q)\sin^2\Delta\theta_{re}\,, \\ L_{\gamma\delta} &= \frac{L_d - L_q}{2}\sin 2\Delta\theta_{re}\,. \end{aligned}$$

It should be noted that the equivalent resistances on d axis and q axis are varied as ω_{rm} increases when $L_{\gamma\delta}$ exists, which is caused by $\Delta\theta_{re}$. As a result, $\Delta\theta_{re}$ forces us to modify the

current controllers (2) – (5) as follows:

$$v_\gamma^* = v_\gamma' - P\omega_{rm}L_q i_\delta \,, \tag{11}$$

$$v_\delta^* = v_\delta' + P\omega_{rm}(L_d i_\gamma + K_E) \,, \tag{12}$$

$$v_\gamma' = \frac{K_{pd}s + K_{id}}{s}(i_\gamma^* - i_\gamma) \,, \tag{13}$$

$$v_\delta' = \frac{K_{pq}s + K_{iq}}{s}(i_\delta^* - i_\delta) \,. \tag{14}$$

3.2 Closed loop system of current control and stability analysis

This subsection analyses robust stability of the closed loop system of current control. Consider the robust stability of Fig.2 to $\Delta\theta_{re}$. Substituting the decoupling controller (11) and (12) to the model (10) if the PWM inverter to feed the IPMSM can operate perfectly (this means $v_\gamma = v_\gamma^*$, $v_\delta = v_\delta^*$), the following equation can be obtained:

$$\begin{bmatrix} v_\gamma' \\ v_\delta' \end{bmatrix} = \begin{bmatrix} R - P\omega_{rm}L_{\gamma\delta} + L_\gamma p & \Delta Z_{\gamma\delta}(p,\omega_{rm}) \\ \Delta Z_{\delta\gamma}(p,\omega_{rm}) & R + P\omega_{rm}L_{\gamma\delta} + L_\delta p \end{bmatrix} \begin{bmatrix} i_\gamma \\ i_\delta \end{bmatrix} + P\omega_{rm}K_E \begin{bmatrix} -\sin\Delta\theta_{re} \\ \cos\Delta\theta_{re} - 1 \end{bmatrix} \,, \tag{15}$$

where $\Delta Z_{\gamma\delta}(p,\omega_{rm})$ and $\Delta Z_{\delta\gamma}(p,\omega_{rm})$ are residual terms due to imperfect decoupling control, and are defined as follows:

$$\Delta Z_{\gamma\delta}(p,\omega_{rm}) = -P\omega_{rm}(L_d - L_q)\sin^2\Delta\theta_{re} + L_{\gamma\delta}p \,,$$

$$\Delta Z_{\delta\gamma}(p,\omega_{rm}) = P\omega_{rm}(L_d - L_q)\sin^2\Delta\theta_{re} + L_{\gamma\delta}p \,.$$

It should be noted that the decoupling controller fails to perfectly reject coupled terms because of $\Delta\theta_{re}$. In addition, with current controllers (13) and (14), the closed loop system can be expressed as shown in Fig.3, the transfer function (16) is obtained with the assumption $p\Delta\theta_{re} = 0$, $p\omega_{rm} = 0$ as follows:

$$\begin{bmatrix} i_\gamma \\ i_\delta \end{bmatrix} = \begin{bmatrix} 1 & F_{\gamma\delta}(s) \\ F_{\delta\gamma}(s) & 1 \end{bmatrix}^{-1} \begin{bmatrix} G_\gamma(s)\cdot i_\gamma^* \\ G_\delta(s)\cdot i_\delta^* \end{bmatrix} \tag{16}$$

where

$$F_{\gamma\delta}(s) = \frac{\Delta Z_{\gamma\delta}(s,\omega_{rm})\cdot s}{L_\gamma s^2 + (K_{pd} + R - P\omega_{rm}L_{\gamma\delta})s + K_{id}} \,,$$

$$F_{\delta\gamma}(s) = \frac{\Delta Z_{\delta\gamma}(s,\omega_{rm})\cdot s}{L_\delta s^2 + (K_{pq} + R + P\omega_{rm}L_{\gamma\delta})s + K_{iq}} \,,$$

$$G_\gamma(s) = \frac{K_{pd}\cdot s + K_{id}}{L_\gamma s^2 + (K_{pd} + R - P\omega_{rm}L_{\gamma\delta})s + K_{id}} \,,$$

$$G_\delta(s) = \frac{K_{pq}\cdot s + K_{iq}}{L_\delta s^2 + (K_{pq} + R + P\omega_{rm}L_{\gamma\delta})s + K_{iq}} \,.$$

Figs.4 and 5 show step responses based on Fig.3 with conventional controller (designed with $\omega_c = 2\pi \times 30$ rad/s) at ω_{rm} =500 min^{-1} and 5000 min^{-1}, respectively. In this simulation, $\Delta\theta_{re}$

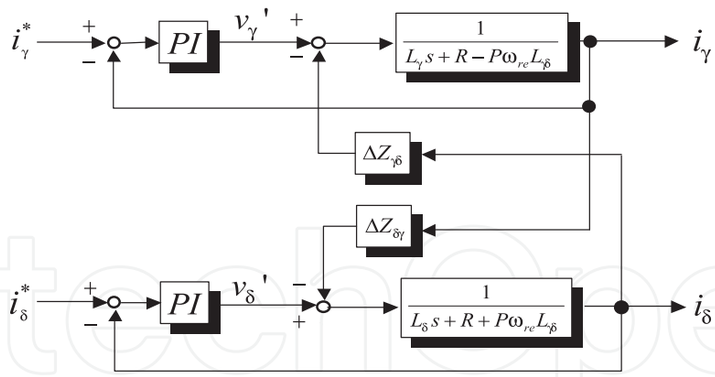

Fig. 3. Closed loop system of current control

Parameters	Value
Rated Power	1.5 kW
Rated Speed	10000 min^{-1}
R	0.061 Ω
L_d	1.44 mH
L_q	2.54mH
K_E	182×10^{-4} V/min^{-1}
P	2 poles

Table 1. Parameters of test IPMSM

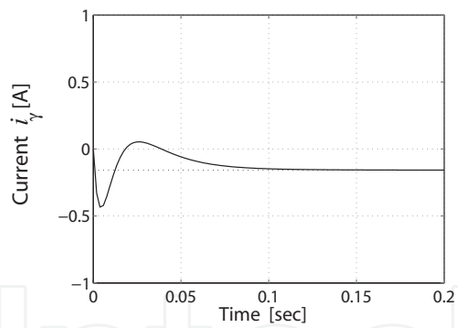

(a) γ axis current response (b) δ axis current response

Fig. 4. Response with the conventional controller ($\omega_{rm} = 500$ min^{-1})

was intentionally given by $\Delta\theta_{re} = -20°$. i_δ^* was stepwise set to 5 A and i_γ^* was stepwise kept to the value according to maximum torque per current (MTPA) strategy:

$$i_\gamma^* = \frac{K_E}{2(L_q - L_d)} - \sqrt{\frac{K_E^2}{4(L_q - L_d)^2} + \left(i_\delta^*\right)^2}\,. \tag{17}$$

The parameters of IPMSM are shown in Table 1. It can be seen from Fig.4 that each current can be stably regulated to each reference. The results in Fig.5, however, illustrate that each current diverges and fails to be successfully regulated. These results show that the current control system tends to be unstable as the motor speed goes up. In other words, currents diverge and

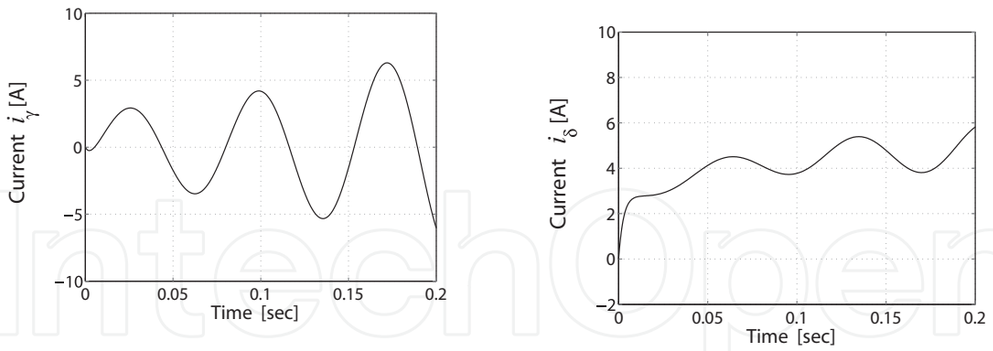

(a) γ axis current response (b) δ axis current response

Fig. 5. Response with conventional controller ($\omega_{rm} = 5000$ min^{-1})

fail to be successfully regulated to each reference in high-speed region because of $\Delta\theta_{re}$, which is often visible in position sensor-less control systems.
Figs.6 and 7 show poles and zero assignment of $G_\gamma(s)$ and $G_\delta(s)$, respectively. It is revealed from Fig.6 that all poles of $G_\gamma(s)$ and $G_\delta(s)$ are in the left half plane, which means the current control loop can be stabilized, and this analysis is consistent with simulation results as previously shown. It should be noted, however, the pole by motor winding is not cancelled by controller's zero, since this pole moves due to $\Delta\theta_{re}$. On the contrary, Fig.7 shows that poles are not in stable region. Hence stability of the current control system is violated, as demonstrated in the aforementioned simulation. This is why one onf the equivalent resistances observed from $\gamma - \delta$ axis tends to become small as speed goes up, as shown in (10), and poles of current closed loop are reassigned by imperfect decoupling control.
It can be seen from $G_\gamma(s)$ and $G_\delta(s)$ that stability criteria are given by

$$K_{pd} + R - P\omega_{rm}L_{\gamma\delta} > 0\,, \tag{18}$$

$$K_{pq} + R + P\omega_{rm}L_{\gamma\delta} > 0\,. \tag{19}$$

Fig.8 shows stable region by conventional current controller, which is plotted according to (18) and (19). The figure shows that stable speed region tends to shrink as motor speed increases, even if position error $\Delta\theta_{re}$ is extremely small. It can also be seen that the stability condition on γ axis (18) is more strict than that on δ axis (19) because of $K_{pd} < K_{pq}$, in which these gains are given by (6) and (8), and $L_d < L_q$ in general. To solve this instability problem, all poles of $G_\gamma(s)$ and $G_\delta(s)$ must be reassigned to stable region (left half plane) even if there exists $\Delta\theta_{re}$. This implies that equivalent resistances in $\gamma - \delta$ axis need to be increased.

4. Proposed current controller with 2DOF structure

4.1 Requirements for stable current control under high-speed region

As described previously, the stability of current control is violated by $\Delta\theta_{re}$. This is because one of the equivalent resistances observed on $\gamma - \delta$ axis tends to become too small, and one of the stability criteria (18) and (19) is not satisfied under high-speed region. To enlarge the stable region, the current controller could, theoretically, be designed with higher performance (larger ω_c). This strategy is, however, not consistent with the aim of achieving lower cost as described in section 1, and thus is not a realistic solution in this case. Therefore, this instability cannot be improved upon by the conventional PI current controller.

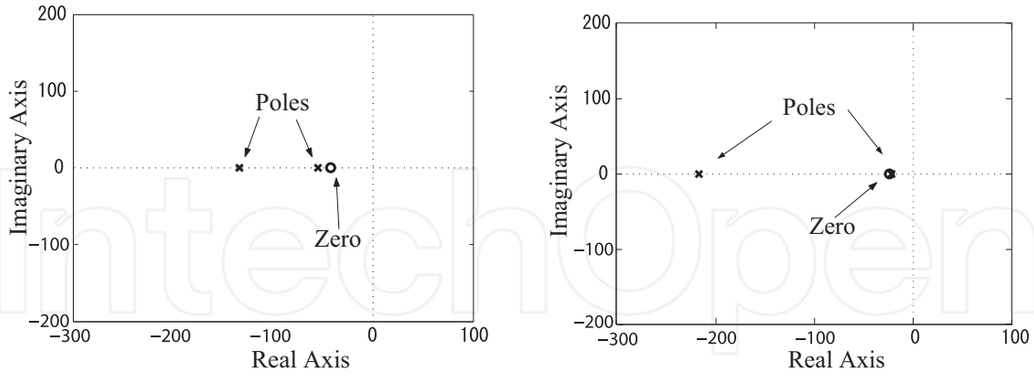

(a) $G_\gamma(s)$ (b) $G_\delta(s)$

Fig. 6. Poles and zero assignment of $G_\gamma(s)$ and $G_\delta(s)$ at $\omega_{rm} = 500$ min^{-1}

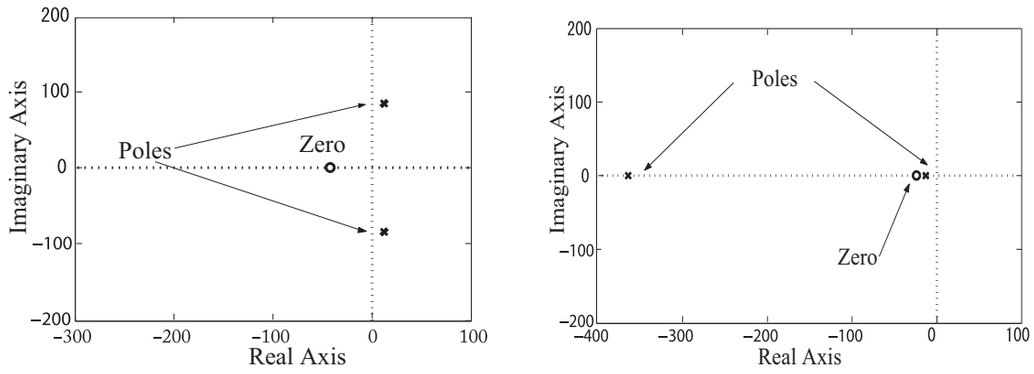

(a) $G_\gamma(s)$ (b) $G_\delta(s)$

Fig. 7. Poles and zero assignment of $G_\gamma(s)$ and $G_\delta(s)$ at $\omega_{rm} = 5000$ min^{-1}

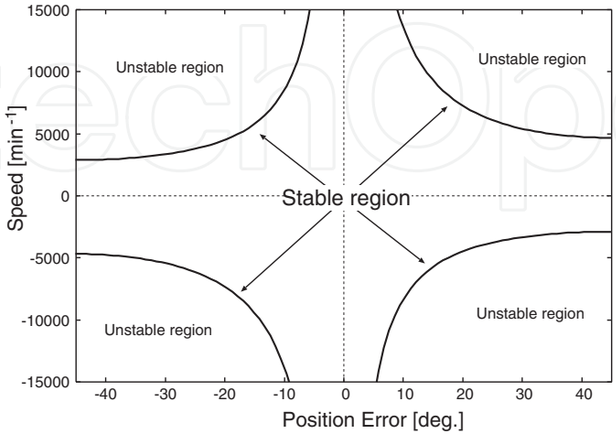

Fig. 8. Stable region by conventional current controller

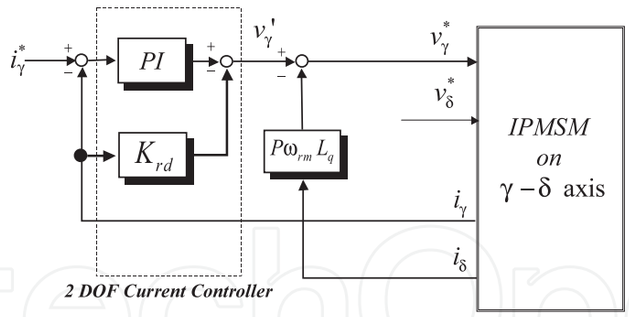

Fig. 9. Proposed current controller with 2DOF structure (only γ axis)

On the other hand, two degree of freedom (2DOF) structure would allow us to simultaneously determine both robust stability and its performance. In this stability improvement problem, robust stability with respect to $\Delta\theta_{re}$ needs to be improved up to high-speed region while maintaining its performance, so that 2DOF structure seems to be consistent with this stability improvement problem of current control for IPMSM drives. From this point of view, this paper employees 2DOF structure in the current controller to enlarge the stability region.

4.2 Proposed current controller

The following equation describes the proposed current controller:

$$v_\gamma' = \frac{K_{pd}s + K_{id}}{s}(i_\gamma^* - i_\gamma) - K_{rd}i_\gamma \ , \tag{20}$$

$$v_\delta' = \frac{K_{pq}s + K_{iq}}{s}(i_\delta^* - i_\delta) - K_{rq}i_\delta \ . \tag{21}$$

Fig. 9 illustrates the block diagram of the proposed current controller with 2DOF structure, where it should be noted that K_{rd} and K_{rq} are just added, compared with the conventional current controller. This current controller consists of conventional decoupling controllers (11) and (12), conventional PI controllers with current control error (13) and (14) and the additional gain on $\gamma - \delta$ axis to enlarge stable region. Hence, this controller seems to be very simple for its implementation.

4.3 Closed loop system using proposed 2DOF controller

Substituting the decoupling controller (11) and (12), and the proposed current controller with 2DOF structure (20) and (21) to the model (10), the following closed loop system can be obtained:

$$\begin{bmatrix} i_\gamma \\ i_\delta \end{bmatrix} = \begin{bmatrix} 1 & F_{\gamma\delta}'(s) \\ F_{\delta\gamma}'(s) & 1 \end{bmatrix}^{-1} \begin{bmatrix} G_\gamma'(s)\cdot i_\gamma^* \\ G_\delta'(s)\cdot i_\delta^* \end{bmatrix}$$

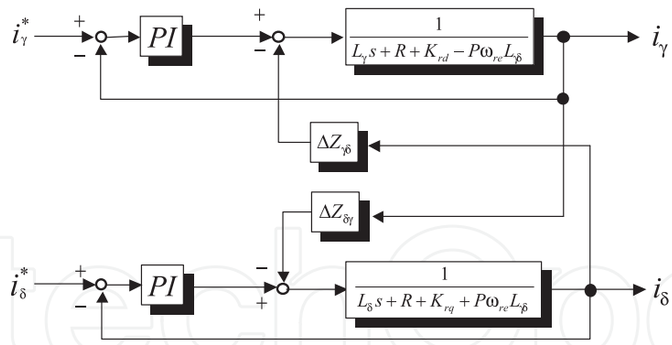

Fig. 10. Current control system with K_{rd} and K_{rq}

where

$$F'_{\gamma\delta}(s) = \frac{\Delta Z_{\gamma\delta}(s, \omega_{rm}) \cdot s}{L_\gamma s^2 + (K_{pd} + K_{rd} + R - P\omega_{rm}L_{\gamma\delta})s + K_{id}} ,$$

$$F'_{\delta\gamma}(s) = \frac{\Delta Z_{\delta\gamma}(s, \omega_{rm}) \cdot s}{L_\delta s^2 + (K_{pq} + L_{rq} + R + P\omega_{rm}L_{\gamma\delta})s + K_{iq}} ,$$

$$G'_\gamma(s) = \frac{K_{pd} \cdot s + K_{id}}{L_\gamma s^2 + (K_{pd} + K_{rd} + R - P\omega_{rm}L_{\gamma\delta})s + K_{id}} ,$$

$$G'_\delta(s) = \frac{K_{pq} \cdot s + K_{iq}}{L_\delta s^2 + (K_{pq} + K_{rq} + R + P\omega_{rm}L_{\gamma\delta})s + K_{iq}} .$$

From these equations, stability criteria are given by

$$K_{pd} + K_{rd} + R - P\omega_{rm}L_{\gamma\delta} > 0 , \tag{22}$$

$$K_{pq} + K_{rq} + R + P\omega_{rm}L_{\gamma\delta} > 0 . \tag{23}$$

The effect of K_{rd} and K_{rq} is described here. It should be noted from stability criteria (22) and (23) that these gains are injected in the same manner as resistance R, so that the current control loop system with K_{rd} and K_{rq} is depicted by Fig.10. This implies that K_{rd} and K_{rq} play a role in virtually increasing the stator resistance of IPMSM. In other words, the poles assigned near imaginary axis ($= -\frac{R}{L_d}, -\frac{R}{L_q}$) are moved to the left ($= -\frac{R+K_{rd}}{L_d}, -\frac{R+K_{rq}}{L_q}$) by proposed current controller, which means that robust current control can be easily realized by designers. In the proposed current controller, PI gains are selected in the same manner as occur in the conventional design:

$$K_{pd} = \omega_c L_d , \tag{24}$$

$$K_{id} = \omega_c (R + K_{rd}) , \tag{25}$$

$$K_{pq} = \omega_c L_q , \tag{26}$$

$$K_{iq} = \omega_c (R + K_{rq}) . \tag{27}$$

This parameter design makes it possible to cancel one of re-assigned poles by zero of PI controller when $\Delta\theta_{re} = 0^\circ$. It should be noted, based this design, that the closed loop dynamics

by the proposed controller is identical to that by conventional controller regardless of K_{rd} and K_{rq}:

$$\frac{i_d}{i_d^*} = \frac{i_q}{i_q^*} = \frac{\omega_c}{s+\omega_c}.$$

Therefore, the proposed design can improve robust stability by only proportional gains K_{rd} and K_{rq} while maintaining closed loop dynamics of the current control. This is why the authors have chosen to adopt 2DOF control.

4.4 Design of K_{rd} and K_{rq}, and pole re-assignment results

As previously described, re-assigned poles by proposed controller ($= -\frac{R+K_{rd}}{L_d}, -\frac{R+K_{rq}}{L_q}$) can further be moved to the left in the $s-$plane as larger K_{rd} and K_{rq} are designed. However, employment of lower-performance micro-processor is considered in this paper as described in section 1, and re-assignment of poles by K_{rd} and K_{rq} is restricted to the cut-off frequency of the closed-loop dynamics at most. Hence, K_{rd} and K_{rq} design must satisfy

$$\frac{R+K_{rd}}{L_d} \leq \omega_c, \tag{28}$$

$$\frac{R+K_{rq}}{L_q} \leq \omega_c. \tag{29}$$

As a result, the design of additional gains is proposed as follows:

$$K_{rd} = -R + \omega_c L_d\ , \tag{30}$$

$$K_{rq} = -R + \omega_c L_q\ . \tag{31}$$

Based on this design, characteristics equation of the proposed current closed loop (the denominator of $G'_\gamma(s)$ and $G'_\delta(s)$) is expressed under $\Delta\theta_{re} = 0$ by

$$Ls^2 + 2\omega_c Ls + \omega_c^2 L = 0,$$

where L stands for L_d or L_q. This equation implies that the dual pole assignment at $s = -\omega_c$ is the most desirable solution to improve robust stability with respect to $\Delta\theta_{re}$ under the restriction of ω_c. In other words, this design can guarantee stable poles in the left half plane even if the poles move from the specified assignment due to $\Delta\theta_{re}$.

4.5 Stability analysis using proposed 2DOF controller

Fig.11 shows stable region according to (22) and (23) by proposed current controller designed with $\omega_c = 2\pi \times 30$ rad/s. It should be noted from these results that the stable speed region can successfully be enlarged up to high-speed range compared with conventional current regulator(dashed lines), which is the same in Fig. 8. Point P in this figure stands for operation point at ω_{rm} =5000 min^{-1} and $\Delta\theta_{re} = -20°$. It can be seen from this stability map that operation point P can be stabilized by the proposed current controller with 2DOF structure, despite the fact that the conventional current regulator fails to realize stable control and current diverges, as shown in the previous step response.

Fig.12 demonstrates that stable step response can be realized under ω_{rm} =5000 min^{-1} and $\Delta\theta_{re} = -20°$. These results demonstrate that robust current control can experimentally be realized even if position estimation error $\Delta\theta_{re}$ occurs in position sensor-less control.

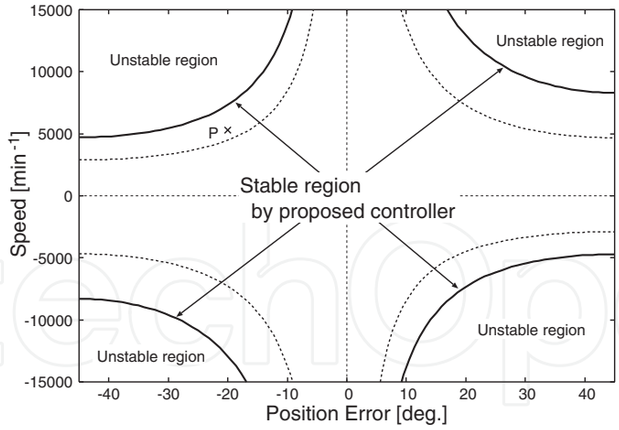

Fig. 11. Stable region by the proposed current regulator with 2DOF structure

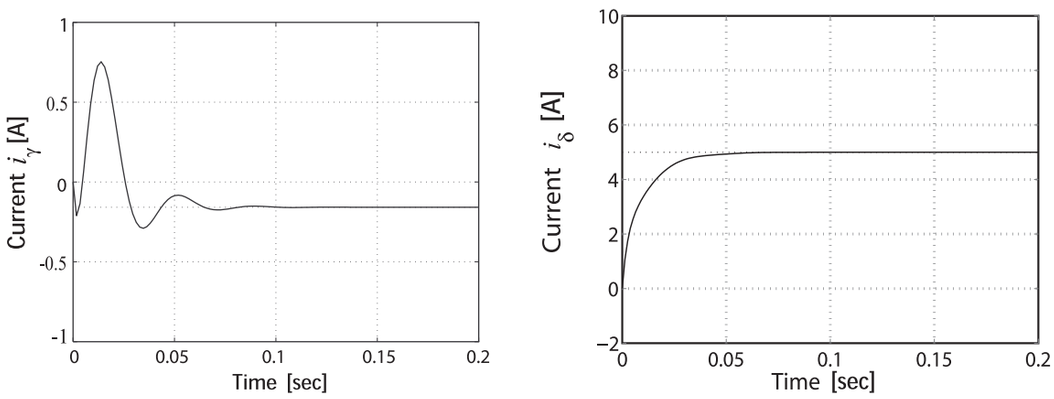

(a) γ axis current response (b) δ axis current response

Fig. 12. Response with proposed controller ($\omega_{rm} = 5000$ min^{-1})

5. Experimental results

5.1 System setup

Experiments were carried out to confirm the effectiveness of the proposed design. The experimental setup shown in Fig.13 consists of a tested IPMSM (1.5 kW) with concentrated winding, a PWM inverter with FPGA and DSP for implementation of vector controller, and position estimator. Also, the induction motor was utilized for load regulation. Parameters of the test IPMSM are shown in Table 1. The speed controller, the current controller, and the coordinate transformer were executed by DSP(TI:TMS320C6701), and the pulse width modulation of the voltage reference was made by FPGA(Altera:EPF10K20TC144-4). The estimation period and the control period were 100 μs, which was set relatively short to experimentally evaluate the analytical results discussed in continuous time domain. The carrier frequency of the PWM inverter was 10 kHz. Also, the motor currents were detected by 14bit ADC. Rotor position was measured by an optical pulse encoder(2048 pulse/rev).

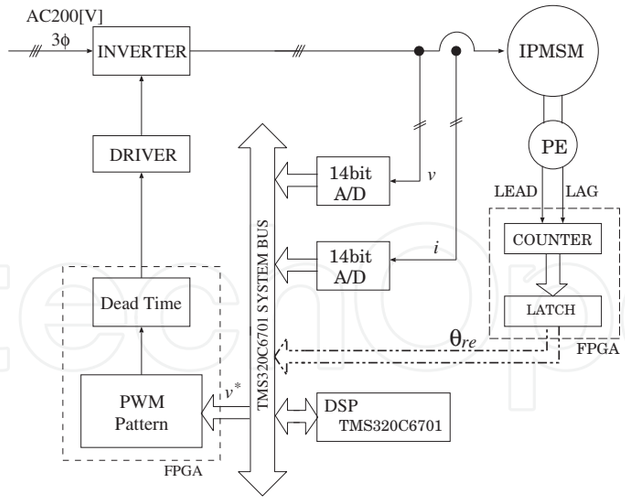

Fig. 13. Configuration of system setup

5.2 Robust stability of current control to rotor position error

The first experiment demonstrates robust stability of the proposed 2DOF controller. In this experiment, the test IPMSM speed was controlled using vector control with position detection in speed regulation mode. The load was kept constant to 75% motoring torque by vector-controlled induction motor. In order to evaluate robustness to rotor position error, $\Delta\theta_{re}$ was intentionally given from 0° to -45° gradually in these experiments.

Figs. 14 and 15 show current control results of the conventional PI controller and the proposed 2DOF controller ($\omega_c = 200\text{rad/s}$) at 4500min^{-1}, respectively. It is obvious from Fig.14 that currents started to be violated at 3.4sec, and they finally were interrupted by PWM inverter due to over-current at 4.2sec. These experimental results showed that $\Delta\theta_{re}$ where currents started to be violated was about -21°, which is consistent with (18) and (19). On the other hand, the proposed 2DOF controller can robustly stabilize current control despite large $\Delta\theta_{re}$ as shown in Fig.15. This result is also consistent with the robust stability analysis discussed in the previous section. Although a current ripple is steadily visible in both experiments, we confirmed that this ripple is primarily the 6th-order component of rotor speed. The tested IPMSM was constructed with concentrated winding, and this 6th-order component cannot be suppressed by lower-performance current controller.

Experimental results at 7000min^{-1} are illustrated in Figs.16 and 17. In the case of conventional controller, current control system became unstable at $\Delta\theta_{re} = -10^\circ$ as shown in Fig.16. Fig.17 shows results of the proposed 2DOF controller, in which currents were also tripped at $\Delta\theta_{re} = -21^\circ$. All $\Delta\theta_{re}$ to show unstable phenomenon is met to (18) and (19), which describes that the robust stability analysis discussed in the previous section is theoretically feasible. This robust stability cannot be improved upon as far as the proposed strategy is applied. In other words, furthermore robust stability improvement necessitates higher cut-off frequency ω_c, which forces us to employ high-performance processor.

5.3 Position sensor-less control

This subsection demonstrates robust stability of current control system when position sensor-less control is applied. As the method for position estimation, the disturbance observer based on the extended electromotive force model (Z.Chen et al. (2003)) was utilized for all experiments. Rotor speed estimation was substituted by differential value of estimated

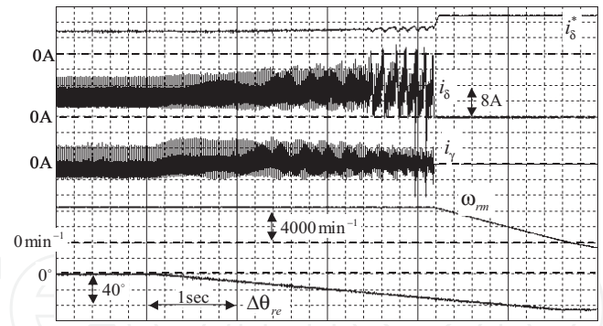

Fig. 14. Current control characteristics by conventional controller at 4500min^{-1}

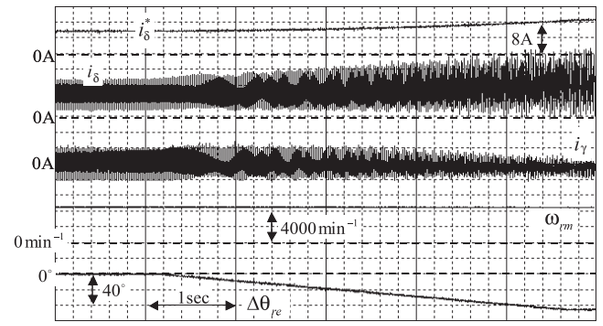

Fig. 15. Current control characteristics by proposed controller at 4500min^{-1}

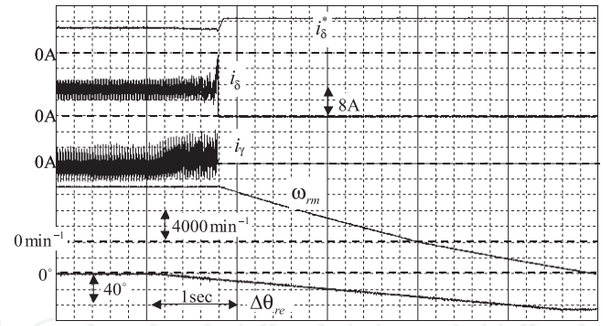

Fig. 16. Current control characteristics by conventional controller at 7000min^{-1}

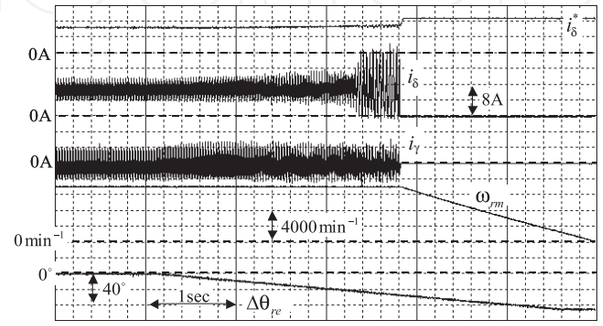

Fig. 17. Current control characteristics by proposed controller at 7000min^{-1}

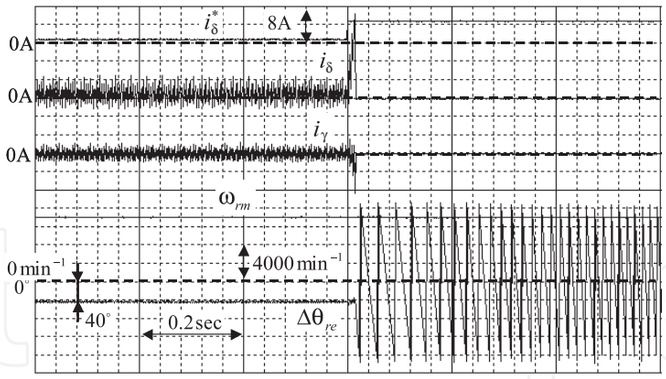

Fig. 18. Current control characteristics by position sensor-less system with conventional controller

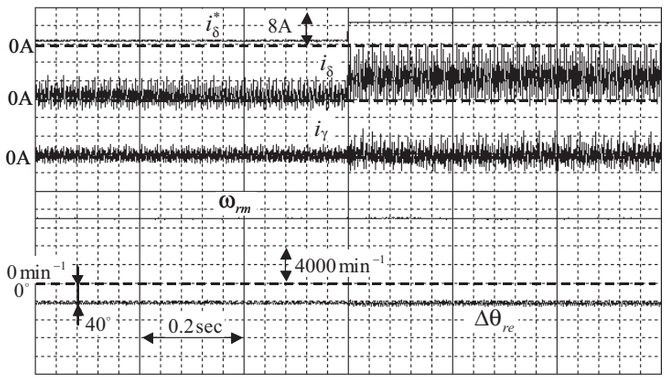

Fig. 19. Current control characteristics by position sensor-less system with proposed controller

rotor position. It should be noted, however, that position estimation delay never fails to occur, especially under high-speed drives, due to the low-pass filter constructed in the disturbance observer. This motivated us to investigate robustness of current control to position estimation delay.

5.3.1 Current step response in position sensor-less control

Figs.18 and 19 show current control results with conventional PI current controller and the proposed controller(designed with $\omega_c = 300\text{rad/s}$), respectively. In these experiments, rotor speed was kept to 7000min^{-1} by the induction motor.

It turns out from Fig.18 that currents showed over-current immediately after current reference i_q^* changed from 1A to 5A, and PWM inverter finally failed to flow the current to the test IPMSM. On the contrary, Fig.19 illustrates that stable current response can be realized even when the current reference is stepwise, which means that the proposed controller is superior to the conventional one in terms of robustness to $\Delta\theta_{re}$.

Also, these figures show that $\Delta\theta_{re}$ of about -40° is steadily caused because of estimation delay in disturbance observer. Needless to say, this error can be compensated since DC component of $\Delta\theta_{re}$ can be obtained in advance according to motor speed and LPF time constant in disturbance observer. $\Delta\theta_{re}$ cannot be compensated, however, at the transient time.

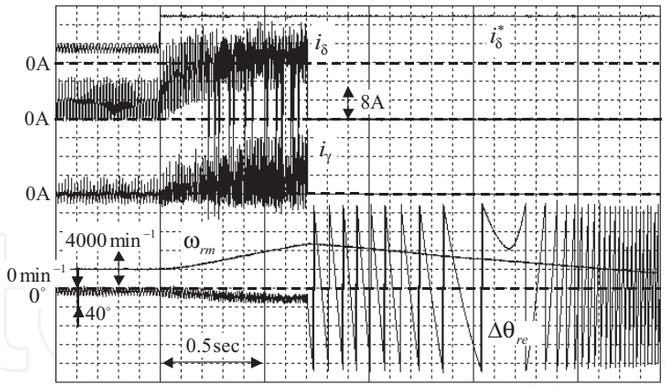

Fig. 20. Speed control characteristics by position sensor-less system with conventional controller

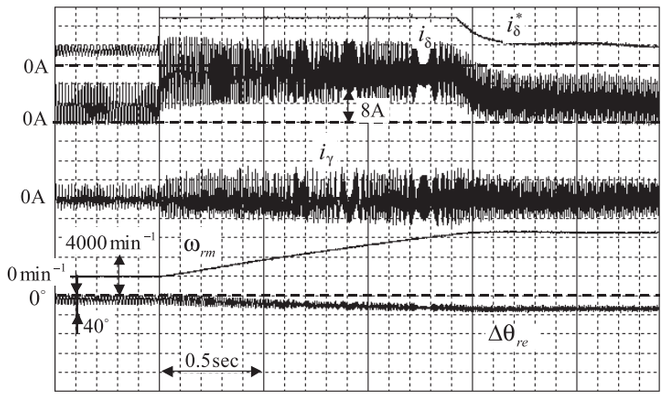

Fig. 21. Speed control characteristics by position sensor-less system with proposed controller

In this study, the authors aimed for robust stability improvement to position estimation error in consideration of transient characteristics such as speed step response and current step response. Hence, $\Delta\theta_{re}$ was not corrected intentionally in these experiments.

5.3.2 Speed step response in position sensor-less control

Figs.20 and 21 show speed step response from $\omega_{rm}^* = 2000\text{min}^{-1}$ to 6500min^{-1} by the conventional PI current controller and proposed controller(designed with $\omega_c = 200\text{rad/s}$), respectively. 20% motoring load was given by the induction motor in these experiments.

It turns out from Fig. 20 that current control begins to oscillate at 0.7sec due to $\Delta\theta_{re}$, and then the amplitude of current oscillation increases as speed goes up. On the other hand, the proposed current controller (Fig. 21) makes it possible to realize stable step response with the assistance of the robust current controller to $\Delta\theta_{re}$.

It should be noted that these experimental results were obtained by the same sensor-less control system except with additional gain and its design of the proposed current controller. Therefore, these sensor-less control results show that robust current controller enables us to improve performances of total control system, and it is important to design robust current controller to $\Delta\theta_{re}$ as well as to realize precise position estimation, which has been surveyed by many researchers over several decades.

6. Conclusions

This paper is summarized as follows:

1. Stability analysis has been carried out while considering its application to position sensor-less system, and operation within stable region by conventional current controller has been analyzed. As a result, this paper has clarified that current control system tends to become unstable as motor speed goes up due to position estimation error.
2. This paper has proposed a new current controller. To guarantee both robust stability and performance of current control simultaneously, two degree of freedom (2DOF) structure has been utilized in the current controller. In addition, a design of proposed controller has also been proposed, that indicated the most robust controller could be realized under the restriction of lower-performance processor, and thus clarifying the limitations of robust performance.
3. Some experiments have shown the feasibility of the proposed current controller with 2DOF structure to realize an enlarged stable region and to maintain its performance.

This paper clarifies that robust current controller enables to improve performances of total control system, and it is important to design robust current controller to $\Delta\theta_{re}$ as well as to realize precise position estimation.

7. References

Hasegawa, M., Y.Mizuno & K.Matsui (2007). Robust current controller for ipmsm high speed sensorless drives, *Proc. of Power Conversion Conference 2007* pp. 1624 –1629.

J.Jung & K.Nam (1999). A Dynamic Decoupling Control Scheme for High-Speed Operation of Induction Motors, *IEEE Trans. on Industrial Electronics* 46(1): 100 – 110.

K.Kondo, K.Matsuoka & Y.Nakazawa (1998 (in Japanese)). A Designing Method in Current Control System of Permanent Magnet Synchronous Motor for Railway Vehicle, *IEEJ Trans. on Industry Applications* 118-D(7/8): 900 – 907.

K.Tobari, T.Endo, Y.Iwaji & Y.Ito (2004 (in Japanese)). Stability Analysis of Cascade Connected Vector Controller for High-Speed PMSM Drives, *Proc. of the 2004 Japan Industry Applications Society Conference* pp. I.171–I.174.

M.Hasegawa & K.Matsui (2008). IPMSM Position Sensorless Drives Using Robust Adaptive Observer on Stationary Reference Frame, *IEEJ Transactions on Electrical and Electronic Engineering* 3(1): 120 – 127.

S.Morimoto, K.Kawamoto, M.Sanada & Y.Takeda (2002). Sensorless Control Strategy for Salient-pole PMSM Based on Extended EMF in Rotating Reference Frame, *IEEE Trans. on on Industry Applications* 38(4): 1054 – 1061.

Z.Chen, M.Tomita, S.Doki & S.Okuma (2003). An Extended Electromotive Force Model for Sensorless Control of Interior Permanent-Magnet Synchronous Motors, *IEEE Trans. on Industrial Electronics* 50(2): 288 – 295.

Robust Control, Theory and Applications

Edited by Prof. Andrzej Bartoszewicz

ISBN 978-953-307-229-6
Hard cover, 678 pages
Publisher InTech
Published online 11, April, 2011
Published in print edition April, 2011

The main objective of this monograph is to present a broad range of well worked out, recent theoretical and application studies in the field of robust control system analysis and design. The contributions presented here include but are not limited to robust PID, H-infinity, sliding mode, fault tolerant, fuzzy and QFT based control systems. They advance the current progress in the field, and motivate and encourage new ideas and solutions in the robust control area.

InTech Europe
University Campus STeP Ri
Slavka Krautzeka 83/A
51000 Rijeka, Croatia
Phone: +385 (51) 770 447
Fax: +385 (51) 686 166
www.intechopen.com

InTech China
Unit 405, Office Block, Hotel Equatorial Shanghai
No.65, Yan An Road (West), Shanghai, 200040, China
中国上海市延安西路65号上海国际贵都大饭店办公楼405单元
Phone: +86-21-62489820
Fax: +86-21-62489821

IntechOpen